Roton-Roton Crossover in Strongly Correlated Dipolar Bose-Einstein Condensates

D. Hufnagl,[1] R. Kaltseis,[1] V. Apaja,[2] and R. E. Zillich[1]

[1]*Institut für Theoretische Physik, Johannes-Kepler Universität, Altenbergerstrasse 69, 4040 Linz, Austria*
[2]*Nanoscience Center, Department of Physics, FIN-40014 University of Jyväskylä, Finland*

(Received 1 May 2011; revised manuscript received 14 June 2011; published 4 August 2011)

We study the pair correlations and excitations of a dipolar Bose gas layer. The anisotropy of the dipole-dipole interaction allows us to tune the strength of pair correlations from strong to weak perpendicular and weak to strong parallel to the layer by increasing the perpendicular trap frequency. This change is accompanied by a roton-roton crossover in the spectrum of collective excitations, from a roton caused by the head-to-tail attraction of dipoles to a roton caused by the side-by-side repulsion, while there is no roton excitation for intermediate trap frequencies. We discuss the nature of these two kinds of rotons and the relation to instabilities of dipolar Bose gases. In both regimes of trap frequencies where rotons occur, we observe strong damping of collective excitations by decay into two rotons.

DOI: 10.1103/PhysRevLett.107.065303 PACS numbers: 67.85.De, 03.75.Kk, 67.85.Hj

Ultracold dipolar Bose gases (DBGs) have become a focus in the study of cold quantum gases [1–3]. Magnetic dipole moments of atoms lead to an anisotropic and long-ranged dipole-dipole interaction. Although small even for high-spin atoms like ^{52}Cr, experiments have shown that the dipole-dipole interaction can influence the shape and stability of a quantum gas [4]. Furthermore, there is much experimental progress in the formation and cooling of dipolar *molecules* [5–11]. Their electric dipole moment can be much larger than magnetic dipole moments, making the dipolar interaction the dominant one. Interesting effects have been predicted such as crystallization without a lattice potential [12,13] or the influence of rotons on the Berezinskii-Kosterlitz-Thouless transition [14].

In the present work we investigate a DBG layer of *finite* thickness, i.e., the limit of a DBG in a pancake-shaped trap with the small trapping frequencies going to zero. Particles can explore the full anisotropy of the dipole-dipole interaction, since the restriction to two dimensions is lifted. The weakly interacting limit of a DBG layer has been studied by using the mean field approximation (Gross-Pitaevskii equation), where indeed dynamical instabilities were found [15,16], accompanied by ''rotonization,'' i.e., the appearance of a local minimum at a characteristic parallel wave number in the dispersion relation. This roton excitation is the soft mode driving the DBG toward instability and can appear at arbitrarily low density if the layer is thick enough. This roton has a completely different physical origin than the roton predicted for a strongly interacting DBG in the two-dimensional limit [17], where it is a consequence of short-range order.

Going beyond the mean field, the hypernetted chain Euler-Lagrange (HNC-EL) method was used in Ref. [18]. Consistent with mean field results, instabilities due to the attractive part of the dipole-dipole interaction were found. Close to the instability, the Bijl-Feynman approximation [19] predicts a roton, and a pronounced peak in the pair distribution function is observed, at a position corresponding to head-to-tail configurations of the dipoles. Here we present calculations of the excitation spectrum based on the correlated basis function Brillouin-Wigner (CBF-BW) method. CBF-BW not only yields an accurate dispersion relation but also takes into account decay processes due to scattering of elementary excitations.

We model a layer of polarized dipoles (pointing in the z direction, having mass m and a short-range isotropic repulsive interaction) in a harmonic trap in the z direction with the Hamiltonian

$$H = \sum_i \left[-\frac{\hbar^2}{2m}\nabla_i^2 + \frac{m\Omega^2}{2} z_i^2 \right] + \sum_{i<j} \left[v_{dd}(\mathbf{r}_{ij}) + \frac{\sigma^{12}}{r_{ij}^{12}} \right] \qquad (1)$$

with $\mathbf{r}_{ij} = \mathbf{r}_i - \mathbf{r}_j$ and where $v_{dd}(\mathbf{r}) = \frac{C_{dd}}{4\pi} \frac{1-3\cos^2\theta}{r^3}$ is the dipole-dipole interaction. We use $(\sigma/r)^{12}$ as a simple model for the repulsion. Our length and energy units r_0 and ϵ_0 are given by $r_0 = \frac{mC_{dd}}{4\pi\hbar^2}$ and $\epsilon_0 = \frac{\hbar^2}{mr_0^2}$, respectively, effectively eliminating the parameters m and C_{dd}. All quantities are expressed in these units and are therefore dimensionless. The parameters of this system are the repulsion σ, the frequency of the confining potential Ω, and the area density n, defined as $n \equiv \int dz \rho(z)$, where $\rho(z)$ is the particle density. Dynamical instability is approached by decreasing σ (which shields the attractive part of the potential), decreasing Ω, increasing n (both increasing the width of the layer), or a combination of the three.

The theoretical basis of HNC-EL and CBF-BW for layer geometries is given in Ref. [20]. The present work is formally similar to studies of ^{4}He confined between walls [21]. In a nutshell, a generalized Jastrow-Feenberg ansatz $\Phi_0 = \exp[\sum_i u_1(z_i) + \sum_{i<j} u_2(z_i, z_j, r_{\parallel,ij})]$ is made for the ground state where $r_{\parallel,ij} = \sqrt{(x_i - x_j)^2 + (y_i - y_j)^2}$ is the parallel distance of two particles. The symmetry of this ansatz follows from the trap geometry (in-plane

translational invariance) as well as from the anisotropy of the dipole-dipole interaction. According to the Ritz variational principle the u_i's are obtained by minimization of the energy: $\delta\langle\Phi_0|H|\Phi_0\rangle/\delta u_i = 0$. For ^{4}He, quantitative results are obtained only by taking into account triplet correlations u_3 and the so-called elementary diagrams E. In the present case of a DBG layer, we set the area density to $n = 2$ for which we will show that u_3 and E have only a small effect even in the worst case of the 2D limit, and we can neglect them. Solving the HNC-EL equations, we obtain the pair distribution function $g(z, z', r_\parallel)$, which follows from division of the probability density to find two particles at perpendicular coordinates z and z' and parallel distance $r_\parallel$ by the one-body densities $\rho(z)$ and $\rho(z')$.

The CBF-BW approximation for excited states [22] can be derived by allowing for time-dependent fluctuations in the above ansatz: $\Psi(t) = e^{-iE_0t/\hbar}\frac{e^{\delta U(t)/2}}{\langle\Psi(t)|\Psi(t)\rangle}\Phi_0$, where $\delta U(t) = \sum_{i=1}^N \delta u_1(\mathbf{r}_i; t) + \sum_{i<j}\delta u_2(\mathbf{r}_i, \mathbf{r}_j; t)$ are fluctuations of the correlations. $\delta U(t)$ is obtained by minimizing the action $S = \int dt\langle\Psi(t)|H - i\hbar\frac{\partial}{\partial t}|\Psi(t)\rangle$ and linearizing the resulting Euler-Lagrange equations. Assuming a perturbing external potential $U_{\text{pert}}e^{-i\omega t}$, we obtain the density-density response operator χ from its definition $\chi^{-1}(\omega)\delta\rho = U_{\text{pert}}$, where $\delta\rho$ is the density fluctuation induced by U_{pert}. In CBF-BW, $\chi(\omega)$ is given by $\chi(\omega) = G(\omega) + G(-\omega)$, where $G(\omega)$ in coordinate representation is given by

$$G(z, z', \mathbf{r}_\parallel; \omega) = \sqrt{\rho(z)\rho(z')}\sum_{m,n}\int d^2k\,\phi_{m,\mathbf{k}}(z)[\varepsilon_n(k) + \Sigma_{mn}(k, \omega) - \hbar\omega - i\eta]^{-1}\phi^*_{n,\mathbf{k}}(z')e^{i\mathbf{k}\mathbf{r}_\parallel}. \quad (2)$$

$\phi_{m,\mathbf{k}}(z)e^{i(k_xx+k_yy)}$ are the Feynman excitation functions for parallel wave vector $\mathbf{k}$ and perpendicular quantum number m, and $\varepsilon_m(k)$ is the excitation energy in the Bijl-Feynman approximation. The dynamic pair correlations δu_2 (absent in the Bijl-Feynman approximation) give rise to the complex self-energy $\Sigma_{mn}(k, \omega)$ [20]. CBF-BW is the minimal variational theory that describes excitation energies and damping qualitatively correctly for strongly correlated systems like ^{4}He. The dynamic structure function is obtained from the fluctuation-dissipation theorem $S(\omega) = -\text{Im}\chi(\omega)/\pi$. Of particular interest are plane wave perturbations with wave vector $\mathbf{k}$, which correspond to Bragg spectroscopy measurements. The resulting $S(\mathbf{k}, \omega) = \int d^3r d^3r' e^{-i\mathbf{k}(\mathbf{r}-\mathbf{r}')}S(z, z', \mathbf{r}_\parallel, \omega)$ is the dissipation cross section for transferring momentum $\mathbf{k}$ and energy $\hbar\omega$ to the system. Thus $S(\mathbf{k}, \omega)$ has a peak whenever $\hbar\omega$ coincides with an excitation energy, and homogeneous broadening of $S(\mathbf{k}, \omega)$ indicates decay of excitations.

We have calculated the ground state and excited states for $\sigma = 0.3$ and area density $n = 2$ and varied the trap frequency Ω. For a system of fermionic KRb molecules [9] these values correspond to the physical parameters $\sigma = 0.18\ \mu$m, $n = 5.32\ \mu\text{m}^{-2}$, and the unit value of the trapping frequency $\Omega_0 = 1.33$ kHz. For the magnetic dipoles of Er_2 [23] these values correspond to $\sigma = 25.4$ nm, $n = 278\ \mu\text{m}^{-2}$, and $\Omega_0 = 26.3$ kHz. Thus, our results are in a parameter regime that is somewhat outside the typical experimental regime. By varying the trap frequency Ω we drastically change the properties of the system. A small value of Ω leads to a wide density profile $\rho(z)$ (shown in the top panel of Fig. 1) with a high probability for head-to-tail configurations, where pairs of particles are located in the attractive well of the dipolar interaction. Increasing Ω decreases this probability, until eventually the DBG becomes two-dimensional. The smallest value of Ω that we achieved was $\Omega = 3.16$, below which the numerical solution of the HNC-EL equations became unstable, as discussed below.

The effect of the trap frequency on the pair distribution $g(z, z', r_\parallel)$ is shown in Fig. 1. In the middle panel, $g(z, z', r_\parallel)$ is plotted for $z = -z'$ and $r_\parallel = 0$ as a function of z. $G_\perp(z) \equiv g(z, -z, 0)$ is a measure of out-of-plane pair correlations. With decreasing Ω, a correlation peak is growing in $G_\perp(z)$, shifted from the classical potential minimum for two particles (indicated by a filled circle) by zero-point motion. Indeed, at $\Omega = 3.16$, $G_\perp(z)$ is elevated above unity for all values of z, which means that particles tend to cluster up atop each other. This is not manifested in the translationally invariant one-body density $\rho(z)$ but only in the pair distribution function. $G_\perp(z)$ even has a second correlation peak at a much larger z value, but $\rho(z)$ is almost zero there. It is this clustering in head-to-tail configurations that brings the DBG closer to instability, as we will see in the excitation spectrum. The lower panel of Fig. 1 shows $G_\parallel(r_\parallel) \equiv g(0, 0, r_\parallel)$, a measure of in-plane pair correlations. Variation of Ω reveals a trend for $G_\parallel(r)$ opposite to $G_\perp(z)$: *Increasing* Ω (i.e., making the system more two-dimensional) increases in-plane correlations. Confining the dipoles shields them from the attractive part of the dipole-dipole interaction. Hence the correlation peak in $G_\parallel(r_\parallel)$ for large Ω is due to the *repulsive* part of the dipole-dipole interaction [and to a smaller degree due to the $(\sigma/r)^{12}$ repulsion]. A comparison between Monte Carlo results [13] and $G_\parallel(r_\parallel)$ in the two-dimensional limit can be found in Ref. [18], where it is shown that for the low area densities used here the HNC-EL method gives very accurate results.

In Fig. 2, we show the main result of this work, the dynamic structure function $S(\mathbf{k}, \omega)$ for a wave vector parallel to the layer ($\mathbf{k} = \mathbf{k}_\parallel$, $k_\perp = 0$). Wave numbers and frequencies are given in units of the trap length, $a_{\text{ho}}^{-1} = \sqrt{\Omega}$ in our units, and the trap frequency Ω, respectively. The Bijl-Feynman approximation $\varepsilon_n(k)$ is shown by dotted lines. The six panels correspond to the different values of Ω used also in the ground state calculations above (again

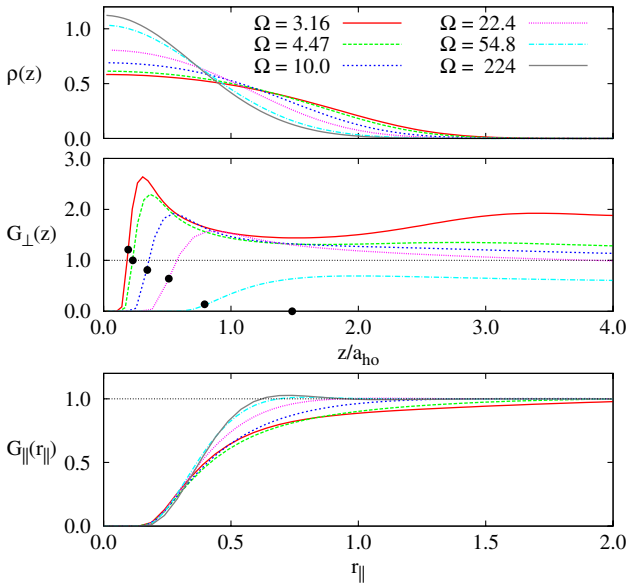

FIG. 1 (color online). Density profile $\rho(z)$ (top panel) and out-of-plane pair distribution $G_\perp(z)$ (middle panel) for several trap frequencies Ω (z is scaled by the oscillator length). As the correlation peak of $G_\perp(z)$ decreases with increasing Ω, a small peak appears in the in-plane pair distribution $G_\parallel(r_\parallel)$ (bottom panel). The location of the potential minimum for two particles is indicated by filled circles.

$\sigma = 0.3$ and $n = 2$). $S(k_\parallel, \omega)$ is shown as a gray-scale map for damped modes. To enhance low intensity regions, the scale is mapped to $S(k_\parallel, \omega)^{1/4}$. Undamped modes lead to δ-like contributions and cannot be displayed in this fashion. Therefore, they are traced by lines in Fig. 2. Since the layer is translationally invariant, parallel momentum is conserved and $\mathbf{k}_\parallel$ is a good quantum number. $S(k_\parallel, \omega)$ probes the dispersion relation of excitations characterized by a wave vector $\mathbf{k}_\parallel$. The strongest signal comes from the excitations with the lowest perpendicular quantum number $\hbar\omega_0(\mathbf{k}_\parallel)$.

Close to instability, at $\Omega = 3.16$, the lowest mode exhibits a roton, i.e., a local minimum in the dispersion relation $\omega_0(\mathbf{k}_\parallel)$ (full line), at a wave number $k_\parallel \approx a_{\mathrm{ho}}^{-1}$. Because of the negative curvature of the dispersion for low $k_\parallel$, the phonon and roton excitations are not damped. When we increase $k_\parallel$ beyond a_{ho}^{-1}, $\omega_0(k_\parallel)$ bends over to form a plateau at twice the roton energy E_r, and the undamped mode loses spectral weight (not visible in Fig. 2, since we refrained from artificial broadening). This effect is well-known for superfluid ^{4}He. It is caused by the high density of states at E_r, leading to a high probability for immediate decay into two rotons, when this decay channel opens at $\hbar\omega = 2E_r$. Beyond a_{ho}^{-1}, more and more spectral weight is carried by a damped, free-particle-like excitation at energies above $2E_r$. We note that $\varepsilon_0(k)$ predicts a value for E_r very similar to CBF-BW. Thus the system is far less correlated than ^{4}He, where CBF-BW is a significant correction to the Bijl-Feynman approximation for the roton energy.

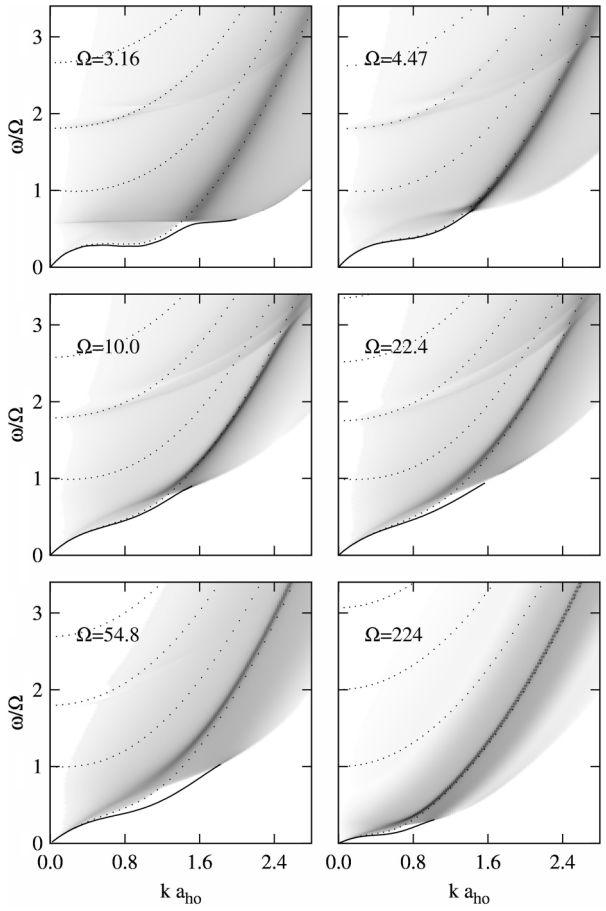

FIG. 2. $S(k_\parallel, \omega)$ for the trap frequency increasing from $\Omega = 3.16$ (top left) to $\Omega = 224$ (bottom right). Undamped modes are shown by lines, and the dotted lines are the excitation energies in the Bijl-Feynman approximation. Roton excitations appear both in the weak and in the strong trapping limit.

The appearance of such a roton in dipole layers was predicted already in the mean field approximation [15,16] and later in the Bijl-Feynman approximation [18]. The mean field calculations have shown that, upon further decreasing Ω, the roton energy E_r can drop to zero, triggering a dynamical instability driven by a perturbation with finite momentum and caused by the dipole-dipole attraction. Unlike the mean field approach, HNC-EL calculations show signs of this instability already in the ground state calculation. Indeed, numerical solution of the HNC-EL equations is exceedingly difficult for smaller Ω, smaller σ, or higher area density n. As explained in Ref. [18], this is an indication that the Jastrow-Feenberg ansatz Φ_0 leads only to a metastable solution even if $E_r > 0$. The true ground state would lie energetically lower than Φ_0. The correlation peak in $G_\perp(z)$ suggests a dimerized phase, where pairs of dipoles are bound [18]. Whether such a phase exists would have to be answered by using either a different ansatz for Φ_0 or a method that does not require a variational ansatz.

Tightening the trap by increasing Ω enhances stability and suppresses the roton and the associated two-roton

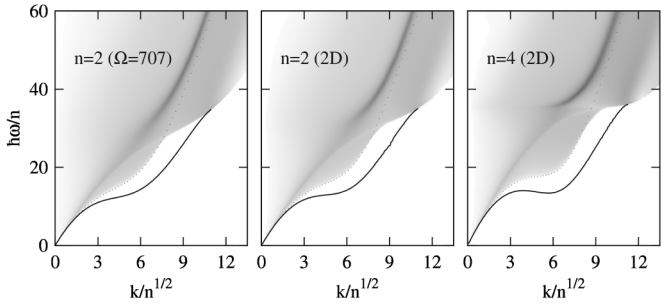

FIG. 3. $S(k_\parallel, \omega)$ for trap frequency $\Omega = 707$ (left panel) and the 2D limit $\Omega = \infty$ (middle panel), with area density $n = 2$. The 2D limit for $n = 4$ is shown in the right panel.

plateau. $\omega_0(\mathbf{k}_\parallel)$ becomes markedly more straight for, e.g., $\Omega = 22.4$. As for $\Omega = 3.16$, also for higher Ω low excitations are undamped for small $k_\parallel$ and become damped when decay into two lower energy modes becomes kinematically possible. For $k_\parallel a_{\rm ho} > 2.4$, decay into perpendicularly excited modes leads to additional broadening. Upon increasing Ω further towards the two-dimensional limit, we observe a *reappearance* of a roton mode, albeit not at $k_\parallel \approx a_{\rm ho}^{-1}$. Between $\Omega = 22.4$ and $\Omega = 54.8$ the bend in $\hbar\omega_0(k_\parallel)$ increases, and at $\Omega = 224$ (bottom right panel in Fig. 2) the dispersion becomes almost flat at $k_\parallel a_{\rm ho} \approx 0.4$, and the in-plane correlation increases; see $G_\parallel(r_\parallel)$ in Fig. 1.

We have calculated the dynamic structure function also in the 2D limit, $S_{\rm 2D}(k, \omega)$, by using precisely the same approximations as for the DBG layer for $\Omega = 224$. We confirmed that $S(k_\parallel, \omega)$ is very similar to the 2D limit $S_{\rm 2D}(k, \omega)$ and becomes indistinguishable for $\Omega = 707$. In the left and middle panels in Fig. 3, we show $S(k_\parallel, \omega)$ for $\Omega = 707$ and $S_{\rm 2D}(k, \omega)$, respectively, as a function of $k/\sqrt{n}$ and $\hbar\omega/n$, which is the more appropriate scaling for a 2D system of density n. The small difference between $S(k_\parallel, \omega)$ and $S_{\rm 2D}(k, \omega)$ is due to including triplets and elementary diagrams in the 2D HNC-EL calculations, which demonstrates that they are indeed of minor importance at $n = 2$. In the right panel, $S_{\rm 2D}(k, \omega)$ is shown at twice the density, $n = 4$. This increases the correlations further and leads to a roton minimum. This is the ''traditional'' roton, as it is also found in ^{4}He films, that results from the short-range order caused by repulsive interactions. The roton wave number is approximately $k_r \approx 6n^{1/2}$, the same value found in Ref. [17] for $\sigma = 0$.

We have demonstrated a roton-roton crossover between two regimes of a DBG layer. (i) In the weak trapping regime, the system is close to an instability due to the head-to-tail attraction of the dipole-dipole interaction. Using HNC-EL, we calculated the pair distribution function, which shows a strong out-of-plane correlation in the weak trapping regime. We obtained the excitation energies from the dynamic structure function in the CBF-BW approximation. The head-to-tail attraction of dipoles leads to a roton minimum at wave number $k_\parallel = a_{\rm ho}^{-1}$ in the lowest collective mode, which is a precursor to dynamical instability and has been found previously by more approximate methods [15,16,18]. The out-of-plane correlation peak and the associated roton vanish upon increasing the trapping strength. (ii) In the strong trapping regime, we find increased in-plane correlations, caused by the side-by-side repulsion of dipoles. In this regime, it is this repulsion and the corresponding short-range order that give rise to a roton at a wave number of about $k_\parallel = 6n^{1/2}$. Thus by tuning the confinement strength, the anisotropy of the dipole-dipole interaction allows us to explore two kinds of rotons with different physical origin: an ''attractive'' roton close to the border to instability and the traditional ''repulsive'' roton.

We are grateful to Eckhard Krotscheck for his help with HNC-EL and to Ferran Mazzanti, Gregory Astrakharchik, and Jordi Boronat for interesting discussions. We also thank Francesca Ferlaino and Rudi Grimm for their hospitality and discussions about experiments on DBGs. We acknowledge financial support by the Austrian Science Fund FWF (Grants No. 21264 and No. 23535).

[1] M. A. Baranov *et al.*, Phys. Rep. **464**, 71 (2008).
[2] *Cold Molecules: Theory, Experiment, Applications*, edited by R. V. Krems, W. C. Stwalley, and B. Friedrich (CRC, Boca Raton, FL, 2009).
[3] T. Lahaye *et al.*, Rep. Prog. Phys. **72**, 126401 (2009).
[4] T. Koch *et al.*, Nature Phys. **4**, 218 (2008).
[5] J. M. Sage *et al.*, Phys. Rev. Lett. **94**, 203001 (2005).
[6] F. Lang *et al.*, Phys. Rev. Lett. **101**, 133005 (2008).
[7] J. G. Danzl *et al.*, Science **321**, 1062 (2008).
[8] S. Ospelkaus *et al.*, Nature Phys. **4**, 622 (2008).
[9] K.-K. Ni *et al.*, Science **322**, 231 (2008).
[10] A.-C. Voigt *et al.*, Phys. Rev. Lett. **102**, 020405 (2009).
[11] K.-K. Ni *et al.*, Nature (London) **464**, 1324 (2010).
[12] H. P. Büchler *et al.*, Phys. Rev. Lett. **98**, 060404 (2007).
[13] G. E. Astrakharchik *et al.*, Phys. Rev. Lett. **98**, 060405 (2007).
[14] A. Filinov, N. V. Prokofev, and M. Bonitz, Phys. Rev. Lett. **105**, 070401 (2010).
[15] L. Santos, G. V. Shlyapnikov, and M. Lewenstein, Phys. Rev. Lett. **90**, 250403 (2003).
[16] D. H. J. O'Dell, S. Giovanazzi, and G. Kurizki, Phys. Rev. Lett. **90**, 110402 (2003).
[17] F. Mazzanti *et al.*, Phys. Rev. Lett. **102**, 110405 (2009).
[18] D. Hufnagl *et al.*, J. Low Temp. Phys. **158**, 85 (2010).
[19] R. P. Feynman, Phys. Rev. **94**, 262 (1954).
[20] B. E. Clements, E. Krotscheck, and C. J. Tymczak, Phys. Rev. B **53**, 12 253 (1996).
[21] V. Apaja and E. Krotscheck, Phys. Rev. Lett. **91**, 225302 (2003).
[22] C. C. Chang and C. E. Campbell, Phys. Rev. B **13**, 3779 (1976).
[23] F. Ferlaino (private communication).